ELSEVIER

Journal of Physics and Chemistry of Solids 60 (1999) 211–221

JOURNAL OF PHYSICS AND CHEMISTRY OF SOLIDS

Characterization of silica nanocomposites obtained by sol–gel process using positron annihilation spectroscopy

Edésia Martins Barros de Sousa[a,*], Welington F. de Magalhães[b], Nelcy D.S. Mohallem[b]

[a]*CDTN/CNEN, Centro de Desenvolvimento da Tecnologia Nuclear, CP: 941, Rua Prof. Mário Werneck s/n, Campus Universitário, Pampulha, Belo Horizonte, MG, Brazil CEP 30123-970*

[b]*Departamento de Química, ICEX, UFMG, Laboratório de Espectroscopia de Aniquilação de Pósitrons, LEAP, C.P. 702, 31270-901 Belo Horizonte, MG, Brazil*

Received 31 March 1998; accepted 19 July 1998

Abstract

SiO_2 matrix was prepared by a sol–gel method using tetraethoxysilane, TEOS, ethanol and water in a 1/3/10 mole ratio, with HCl and HF as catalysts. This silica gel was doped with copper with different precursors and different contents of dopant. The samples were prepared into monolithic shape, dried at 110°C for 24 h and thermally treated for 2 h at 500, 900 and 1100°C. The structural evolution was studied by positron annihilation lifetime spectroscopy (PALS) which has been shown to be a useful tool for pore size analysis in several materials, X-ray diffraction (XRD) and nitrogen gas adsorption. All the samples have shown, according to the positron spectroscope results, a stable pore structure up to 900°C and a strong densification process at 1100°C.

Keywords: B. Sol–gel growth; C. Positron annihilation spectroscopy

1. Introduction

The sol–gel method [1, 2] to produce glasses, ceramics and glass–ceramics has been utilized for a variety of products ranging from optical fibers, lenses, and special coatings to the production of ultra-pure powders. The sol–gel method allows a nanostructural control of ceramics, based on the performance upon the formation and evolution of nanometric units through process variables. Materials obtained by this process present high surface area and chemical composition homogeneity [3, 4]. By this process it is possible to obtain composite materials through incorporation of small amounts of different components in the ceramic matrix, at low temperatures, because it deals with liquid reagents and network development by chemical reaction [5].

Several ceramic composites have been obtained for a wide variety of applications. Silica matrix embedded with copper particles exhibits important properties in catalysis, sensors, electronics, etc. The catalytic oxyhydrochlorination by supported copper chloride has been much studied [6]. In earlier work on copper catalysis, several factors promoting alkane formation were the subjects of research. Nowadays, alternatives for copper-chromite catalysis are the subject of extensive research and copper–silica-based catalysts have been described in the scientific literature [7, 8]. However, the sol–gel process allows the dissolution of the salt into the silica matrix, which results in a mechanically more stable catalyst. This material can probably be used for longer, when compared with silica-supported copper catalysts prepared by precipitation of salt onto silica particles. According to Duval et al. [9], silica gels doped with copper become ferromagnetic after heating and baking up to 400–800°C. This fact is probably a consequence of the cluster shape and of the interation of Cu^{2+} ions with the silica. The third-order optical nonlinearity of the Cu-doped silica is becoming an important area of research, and hence attracting renewed interest from the perspective of production of the metal-doped glasses [10, 11]. The incorporation of copper ions into silica glass prepared by the sol–gel method allows the establishment of a coloring mechanism by the change of oxidizing state. The structural characterization of these materials is of fundamental importance for the

* Corresponding author. Fax: + 31-499-33990; e-mail: sousaem@urano.cdtn.br

0022-3697/99/$ - see front matter
PII: S0022-3697(98)00263-7

control of the processing and final properties of these materials.

Different techniques have been used for morphological characterization, such as pore diameters. Positrons have been used as a nano-probe by PALS, in order to investigate the free volume (V_f) in several materials [12, 13]. When a positron enters a condensed medium, it may annihilate directly with an electron, or it may capture an electron to form a hydrogen-like atom, called positronium, Ps. Positronium can exist in two forms: para-positronium, p-Ps, and ortho-positronium, o-Ps. The p-Ps is the singlet state with total spin of zero. It has a self-annihilation lifetime in vacuum of 0.125 ns and decays via two gamma emissions. The o-Ps is the triplet state with a total spin of one. Its free space lifetime is much longer, 140 ns, and decays via three gamma emissions [14]. In this way, o-Ps survives long enough to interact with surrounding atomic and molecular electrons. This interaction leads to the shortening of its lifetime and to an annihilation with two gamma emission through the process called pick-off annihilation. Measurement of this o-Ps shortened lifetime can thus yield information about the physical and chemical properties of the medium.

The annihilation rate of the different positron species (λ_i), is given by:

$$\lambda_i = \tau_i^{-1} = \text{const} \times \int \rho_-(r) \cdot \rho_+(r) dr \quad (1)$$

where $\rho_-(r)$ and $\rho_+(r)$ are the density of the electron and positron at position r, respectively, and the parameter 'const' is the normalization constant related to the number of the electrons involved in the annihilation. According to the free volume model for o-Ps pick-off annihilation, Ps is confined to a rigid spherical potential well, its mean lifetime depends on the radius, R, of this free volume following the equation [13–15]:

$$\frac{1}{\lambda_3} = \tau_3 = 0.5 \text{ ns} \left[1 - \frac{R}{R_0} + \sin \frac{1}{2\pi} \left(\frac{2\pi R}{R_0} \right) \right]^{-1} \quad (2)$$

where $\Delta R = R_0 - R = 1.656$ Å corresponds to the width of the electron layer of the atoms of the material that penetrates inside the potential well of radius R_0, in which one Ps acts and annihilates by pick-off. As by hypothesis o-Ps is confined to the spherical free volume, the relation between R and V_f is given by:

$$V_f = 4\pi R^3/3 \quad (3)$$

In this work SiO_2 matrixes were prepared by the sol–gel process and doped with copper salts. This work was intended to analyze the structural evolution of Cu-doped porous silica gels through PALS, XRD and BET techniques following specific thermal treatments.

2. Experimental

The SiO_2 matrix was prepared by the sol–gel method using TEOS, ethanol and water in a 1/3/10 molar ratio, with HCl and HF as catalysts. These silica gels were doped with copper adding CuCl or $CuSO_4$, at different copper content (1 and 5 mol%), in the starting solution, during agitation. The samples were prepared in monolithic shape, dried at 110°C for 24 h and thermally treated for 2 h at 500, 900 and 1100°C.

The structural evolution was studied by XRD in a RIGAKU Geigerflex 3034 apparatus using a curved crystal monocromator of graphite. All measurements were recorded with 40 kV voltage and 30 mA current at room temperature. The pore characteristics of the samples were analyzed by using a nitrogen gas adsorption machine type Autosorb (Quantachrome Nova 1200), which is an automated physical adsorption system that provides accurate equilibrium adsorption and desorption. Nitrogen gas was used for approx. 5 h with a 22-point adsorption–desorption cycle. The adsorber or desorbed volume data points obtained at various relative pressure are reduced to produce surface area, pore size distribution, micropore volume and average pore radius by BET. The samples were outgassed for 3 h at 200°C.

PALS measurements were carried out using a fast–fast coincidence system (ORTEC), with a time resolution of 280 ps, from the ^{60}Co prompt curve. The ^{22}Na positron source, with 4.0×10^5 Bq activity, was sandwiched between two 7 μm thick foils of KAPTON. Lifetime spectra were resolved into three components, by the POSITRONFIT-EXTENDED [16] program. In the lifetimes, τ_i, and associated intensities, I_i, the subscripts $i = 1$, 2 and 3 refer to p-Ps, the free positron and o-Ps, respectively, and the superscript '0' refers to parameters obtained for the pure matrix. The errors of the PAL parameters are nearly in the range of $s(\tau_3) \cong 3$–5 ns and $s(I_3) \cong 0.5$–1.5%. These errors are standard deviations estimated from three or more spectra of each sample obtained in the POSITRONFIT-EXTENDED analysis.

3. Results and discussion

3.1. Sample preparation

After the drying stage, monolithic porous gels samples were obtained without macroscopic defects. The samples remained undamaged after the different thermal treatments. The dried matrixes were transparent above 500°C. The doped gels, initially green, changed from the original color to blue at 500°C and then dark brown at 900°C. At 1100°C, the samples doped with CuCl presented a black color, and that one doped with $CuSO_4$, presented a dark yellow color.

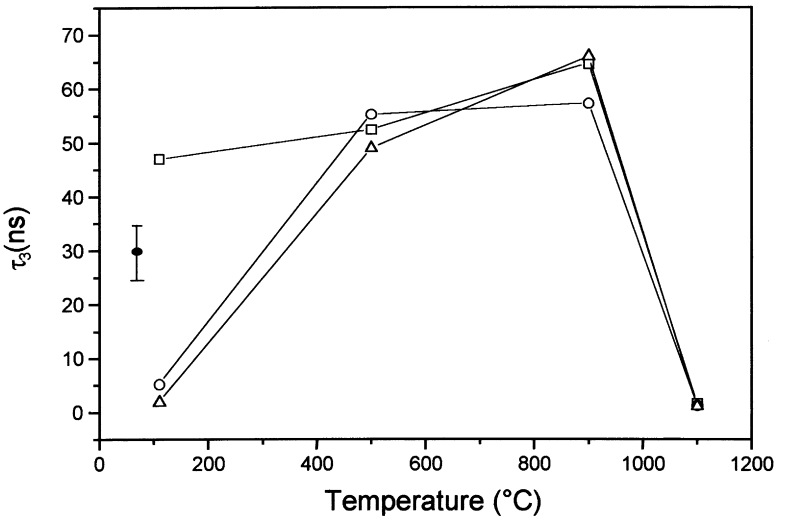

Fig. 1. Variation of o-Ps lifetime of the pure silica matrix (□), doped with 1% (○) and 5% (△) CuCl, as a function of temperature.

3.2. Positron annihilation lifetime spectroscopy (PALS)

The PALS parameters for the compounds obtained are shown in Table 1, determined from the spectra analyses with three components (exponential decay) fixing the lifetime of p-Ps at 0.120 ns.

Fig. 1 shows the variation of the o-Ps lifetime formed in the matrix doped with 1 and 5% of CuCl as a function of different thermal treatments. By analyzing the results of the pure silica matrix, it is observed that the o-Ps lifetime, τ_3, in this material, treated below 1100°C, is high and almost constant. A significant decrease of τ_3 is observed at 1100°C. These results suggest that at this temperature an intense decrease in the free volume size occurs, according to values of the free volume radii and average free volume size, obtained by Eq. (2) and Eq. (3), respectively, and are shown in the Table 1.

For the binary systems containing 1 and 5% of the CuCl, the general behavior is similar to that in silica matrix, except for the composites dried at 110°C. In this case, τ_3 takes values as small as those found in the composites densified at 1100°C. This result is attributed to a chemical effect promoted by the copper ions dissolved into the matrix which reduce the o-Ps lifetime by an o-Ps oxidation reaction

$$\begin{array}{ccc} o-Ps + Cu^{x+} & \xrightarrow{k_{ox}} & e^+ + Cu^{(x-1)+} \\ \downarrow \tau_3^o & & \downarrow \tau_2^o \\ 2\gamma & & 2\gamma \end{array}$$

This reaction transforms the long lifetime species into another of smaller lifetime. This process is known as Ps quenching. The efficiency of this process increases with the concentration, C, of the quencher and depends on the reaction rate constant, k_{ox}. In these cases, it could be shown that a τ_3 decrease is expected with the increasing C according to:

$$(\tau_3)^{-1} = (\tau_3^o)^{-1} + k_{ox}C \quad (4)$$

where τ_3^o is the o-Ps lifetime in the pure matrix. A decrease of τ_3 effectively observed in the dried samples at 110°C confirms the chemical attribution of the quenching effect; thus, the small values of τ_3 in these samples could not be associated with the small size of the pores.

The high values of the τ_3 observed in the samples doped with CuCl, after thermal treatment at 500 and 900°C, can be understood by either or both of the following hypotheses:

- a change in the chemical state of the copper ions leading it to chemically inactive form from the perspective of Ps inhibition and quenching;
- a segregation of these ions to a second phase of copper oxide, transforming a solid solution into a biphasic system after thermal treatment. In this case, as the system is practically pure silica phase, the τ_3 values are almost that of the pure matrix.

Fig. 2 shows the variation of the o-Ps lifetime formed in the pure matrix and doped with 1 and 5% of $CuSO_4$ as a function of different thermal treatments. As the relation between the pore radius, R, and τ_3 is almost linear in the range of right τ_3, the variation of R as a function of the heating temperature has the same pattern, except for the samples doped with 1% of $CuSO_4$ at 110°C (and also 1 and 5% of CuCl at 110°C), as depicted in Fig. 2 (and also Fig. 1). By analyzing the results of the sample doped with 1% of $CuSO_4$, it could be verified that the general behavior is the same as that observed for the samples doped with 1 and 5% of CuCl; that is, τ_3 presents short values at 110°C which are related to the quenching discussed previously.

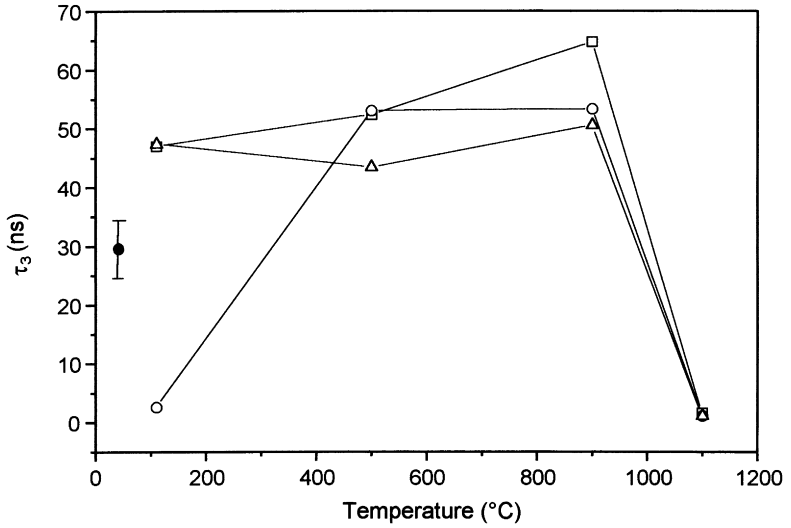

Fig. 2. Variation of o-Ps lifetime of the pure silica matrix (□), doped with 1% (○) and 5% (△) of $CuSO_4$, as a function of temperature.

However, for the system with 5% of $CuSO_4$ content, this behavior is not verified at 110°C. Here, τ_3 presents a high value similar to those of pure silica in the same condition. This fact could be related to the immiscibility of the salt in this system during the sol preparation, gelation or drying process. The segregation of the salt could have occurred in a second phase leading to a silica network free of the copper ions, known as Ps inhibitor and quencher. Once the dopant content is low, the volume fraction of this salt phase is very small when compared with that of the silica phase. This results in a low probability of finding the injected positron in the salt phase. In this salt phase, no Ps formation is expected, as is the case in all ionic solids, and all the Ps formed in the system comes from the silica phase.

When the density and the positron linear absorption coefficient (or positron penetration profile) of both phases are comparable, the o-Ps yield, I_3, is a linear function of the

Table 1
PALS parameters for the silica composites with different composition and thermal treatment temperatures and free volume radii and volume

Sample	T (°C)	τ_3 (ns)	I_3 (%)	R (Å)	$V_f \times 10^{-4}$ (Å^3)
Matrix	110	46.97	28.98	12.32	0.7834
	500	52.35	33.48	12.84	0.8876
	900	64.69	47.04	13.92	1.1304
	1100	1.54	53.72	2.38	0.0057
Si–1% CuCl	110	5.21	11.23	—	—
	500	55.24	27.14	13.11	0.9441
	900	57.21	32.14	13.29	0.9827
	1100	1.21	42.37	1.70	0.0032
Si–5% CuCl	110	1.82	2.14	—	—
	500	48.93	16.28	12.52	0.8212
	900	65.89	12.14	14.02	1.1542
	1100	1.08	48.26	1.78	0.0024
Si–1% $CuSO_4$	110	2.60	11.52	—	—
	500	53.00	18.92	12.91	0.9003
	900	53.35	21.51	12.94	0.9071
	1100	1.10	67.19	1.81	0.0025
Si–5% $CuSO_4$	110	47.36	14.88	12.36	0.7909
	500	43.36	10.30	11.95	0.7140
	900	50.49	22.37	12.67	0.8515
	1100	1.07	44.84	1.77	0.0023

Table 2
Structural characteristics of the samples studied at different temperatures obtained by mercury porosimetry (measurements are accurate to within 7%)

Sample	T (°C)	ρ_{pic} (g/cm^3)	ρ_{por} (g/cm^3)	Porosity (%)	Radio (Å)
Matrix	110	0.63	0.92	38	54
	500	0.58	0.90	52	53
	900	1.89	1.94	42	50
	1100	2.14	—	4	—
Si–1% CuCl	110	0.70	1.25	46	62
	500	0.68	1.01	51	65
	900	0.83	1.29	46	68
	1100	1.89	—	5	—
Si–5% CuCl	110	0.87	1.19	45	64
	500	0.74	1.17	52	61
	900	1.10	1.32	32	58
	1100	1.17	—	7	—
Si–1% $CuSO_4$	110	0.74	0.94	45	66
	500	0.69	0.91	47	67
	900	0,95	1.34	43	61
	1100	1.54	—	9	—
Si–5% $CuSO_4$	110	0.72	1.13	30	63
	500	0.70	0.79	48	59
	900	0.74	1.14	28	62
	1100	0.98	—	11	—

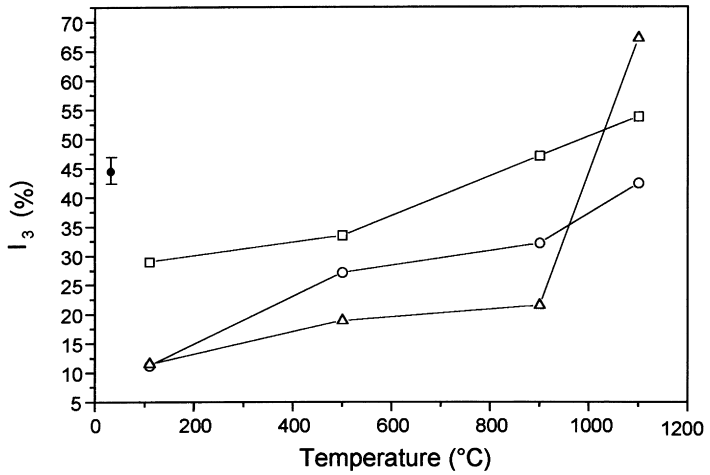

Fig. 3. Variation of o-Ps intensity of the pure silica matrix (□), doped with 1% of CuCl (○) and 1% of $CuSO_4$ (△) as a function of temperature.

contents of the phase forming Ps, and τ_3 is independent of the dopant content and equal to that of the phase forming Ps [15]. In our case the salt phase has a higher density ($\rho_{(CuSO_4.5H_2O)} = 2.28$ g/cm^3) than the silica phase (Table 2) and certainly a higher positron absorption coefficient. Under this condition a lower I_3 is expected than that predicted by the linear relation, as was observed (Table 1).

In these materials a crescent intensity of the o-Ps formation I_3 was observed, whose temperature reached a maximum value at 1100°C. Fig. 3 shows the variation of the intensity of the o-Ps formation I_3 in the pure matrix and doped with 1% of CuCl and 1% of $CuSO_4$ as function of the different temperatures. The decrease of I_3 with the increase in CuCl concentration is consistent with a process of total inhibition with a inhibition constant of nearly 2 (mol%)$^{-1}$ at 110°C, 0.22 (mol%)$^{-1}$ at 500°C and 0.52 (mol%)$^{-1}$ at 900°C. Thus, between 900 and 1100°C the average free volume size strongly decreases and the number or concentration of free volumes increases with the heat thermal treatment.

In the system doped with $CuSO_4$, there is no clear behavior for the inhibition effect as a function of salt concentration. This result is evidence for the complex behavior of the $SiO_2/CuSO_4$ composite concerning its structure and reactivity towards positronium and their precursors.

3.3. XRD characterization

For the SiO_2 matrix treated up to 1100°C, the XRD patterns exhibit amorphous behavior. However, an increase in the intensity and a narrowing in the diffraction band is observed with increasing temperature. This fact indicates an

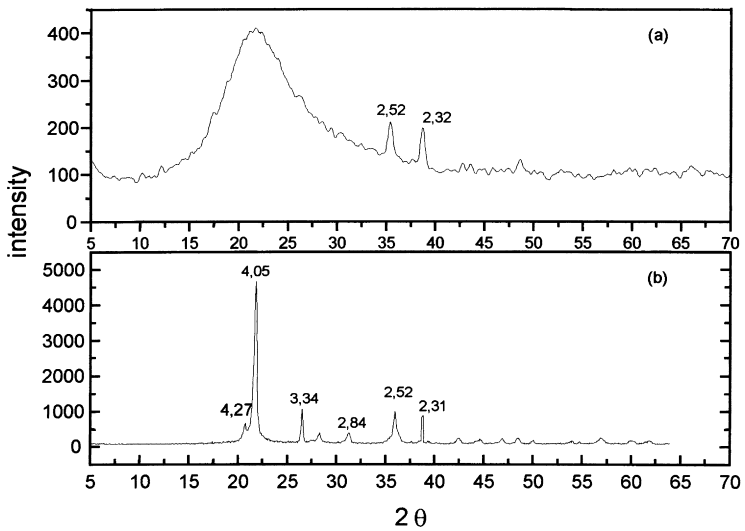

Fig. 4. X-ray diffraction patterns for the samples doped with 5% CuCl and heat at (a) 900°C; and (b) 1100°C.

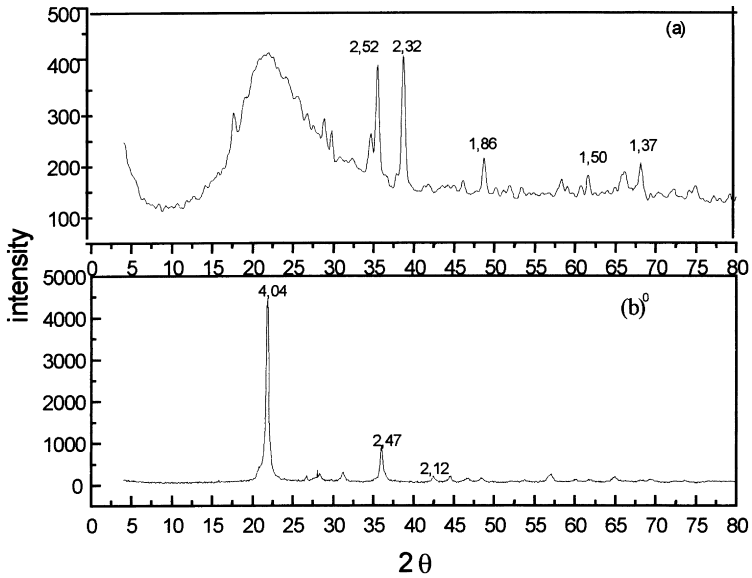

Fig. 5. X-ray diffraction patterns for the samples doped with 5% $CuSO_4$ and heat at (a) 900°C; and (b) 1100°C.

increase in the tetrahedron organizations of the silica samples. For the binary systems, Fig. 4 and Fig. 5 show the evolution of X-ray patterns of samples doped with 5% of CuCl and $CuSO_4$, respectively, treated at 900 and 1100°C. The results show traces of the crystallization of silica gel by diffraction peaks of quartz and cristobalite at 1100°C. It could be observed that the introduction of the dopants in silica gels results in the crystallization of the glass. SiO_2 matrix with 5% content of CuCl exhibits amorphous behavior up to 500°C. The very weak diffraction peaks present at 900°C were attributed to the crystal structure of tenorite, CuO. However, a significant effect was verified as the sample was treated at 1100°C. At this temperature, the amorphous matrix converts to cristobalite and quartz

Table 3
Average values of the structural characteristics of the samples at different temperatures obtained by BET (measurements are accurate to within 5%)

Sample	T (°C)	Area (m^2/g)	Pore size (Å)	$V_p \times 10^3$ (cm^3/Å)	Micro area ($m^2\ g^{-1}$)	Meso Area ($m^2\ g^{-1}$)
Matrix	110	382	16.89	171	243	101
	500	484	17.10	445	341	143
	900	10.68	7.44	0.131	0.35	0.33
	1100	—	—	—	—	—
Si–1% CuCl	110	306	16.95	161	214	91.0
	500	442	17.02	274	358	84.0
	900	8.21	12.73	3.02	4.74	3.47
	1100	1.11	5.0	0.83	0.73	0.38
Si–5% CuCl	110	312	12.15	189	279	32.0
	500	485	15.53	251	401	84.0
	900	40	12.13	25	33	6.28
	1100	4.42	7.42	3.85	3.37	1.05
Si–1% $CuSO_4$	110	293	15.68	408	213	79.0
	500	318	16.92	409	194	124
	900	159	11.73	172	90.2	69.0
	1100	6.47	5.03	1.76	3.73	2.71
Si–5% $CuSO_4$	110	254	12.08	196	237	17.0
	500	351	16.93	611	313	39.0
	900	163	13.91	143	94	69.0
	1100	8.36	5.21	10.55	4.26	4.10

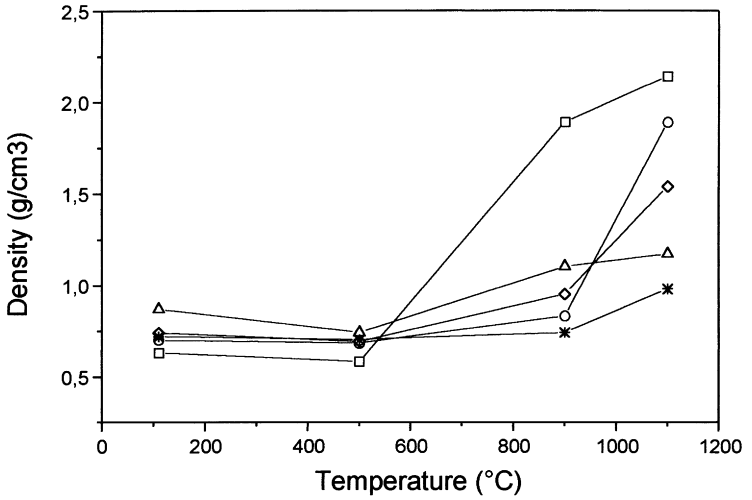

Fig. 6. Variation of density as a function of temperature for silica matrix (□), doped with 1 (○) and 5% (△) CuCl and 1 (◇) and 5% (*) $CuSO_4$.

beyond to favor the crystallization of the tenorite. The X-ray patterns of samples containing 5% of $CuSO_4$ show the decrease in the content of amorphous silica with the increase in temperature. At 110 and 500°C, the $CuSO_4.5H_2O$ phase was detected, which could be related to the immiscibility of the salt at the sol preparation. This fact indicates the probability of the concentration being near or above the solubility of $CuSO_4$ in this system. At 900°C, typical peaks of the copper oxide, CuO can be observed. The X-ray patterns at 1100°C show a set of feature peaks of different silica phases, cristobalite and quartz, of CuO, besides suggesting the appearance of the second phase of the copper oxide, Cu_2O. This phase is not very distinct in the X-ray patterns because their most intense peaks are near or over those of the crystalline silica. This fact made the identification of the Cu_2O in this sample difficult. However, this was further corroborated with EXAFS according to the study by Sousa [17].

3.4. Structural characteristics measured by BET and mercury porosimetry

The structure of the gel strongly depends on the experimental conditions during the hydrolysis reaction, that is, water/precursors ratio, type and concentration of catalysts, temperature, and so on. When the gels are produced by the complete hydrolysis in solution, the dried gels can present a high concentration of hydroxyl

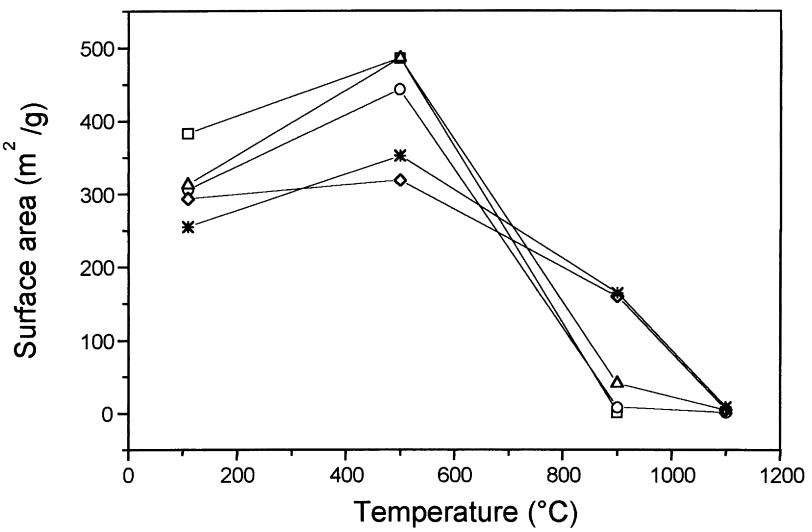

Fig. 7. Variation of surface area as a function of temperature for silica matrix (□), doped with 1 (○) and 5% (△) CuCl and 1 (◇) and 5% (*) $CuSO_4$.

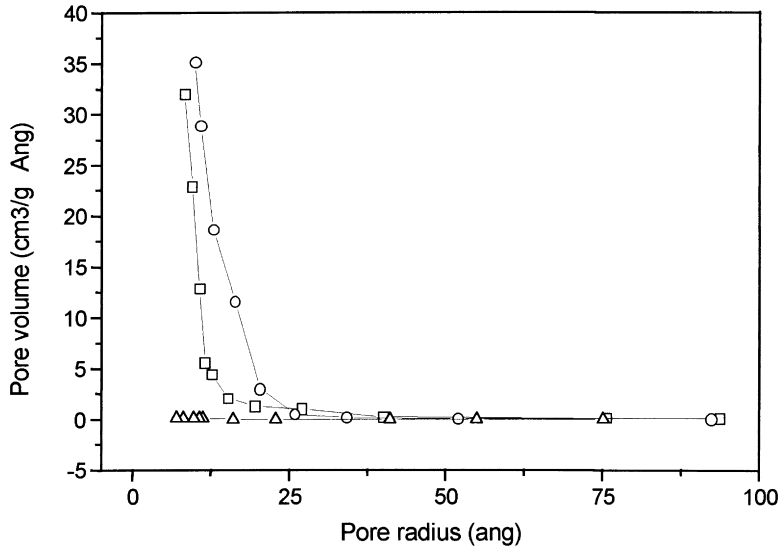

Fig. 8. Pore size distribution from the BET for the pure silica sample at (□) 110°C; (○) 500°C; and (△) 900°C.

groups chemically bonded, due to the re-esterification reaction during the dry process. As the gels are heated, the alkoxy groups and the hydroxyl groups are removed by condensation reaction, which provokes substantial weight loss in the material. These reactions produce cross-linking and consequently gel network shrinkage or densification occur.

Table 2 shows the values of the structural characteristics obtained by mercury porosimetry and picnometry for dried samples and treated at 500, 900 and 1100°C. In this table, ρ_{pic} and ρ_{por} represent volumetric density of picnometry and porosimetry, respectively. The surface area, average pore size, pore size distribution and total pore volume were obtained through BET. These results are shown in Table 3, for the samples treated at different temperatures.

The organic retained and the dopants added to the xerogel can exert effects on the structure of the material. The density measured by picnometry and the surface area measured by BET of different samples are shown in Fig. 6 and Fig. 7, respectively as a function of the temperature. Analysis of the values obtained, reveals that the density of the gels decreases at 500°C. At this temperature, the surface area and the porosity present maximum values. At 110°C, the pure silica samples were yellowish, probably due to the organic impregnation at the network. As the samples were treated at 500°C, the organics were removed and the samples

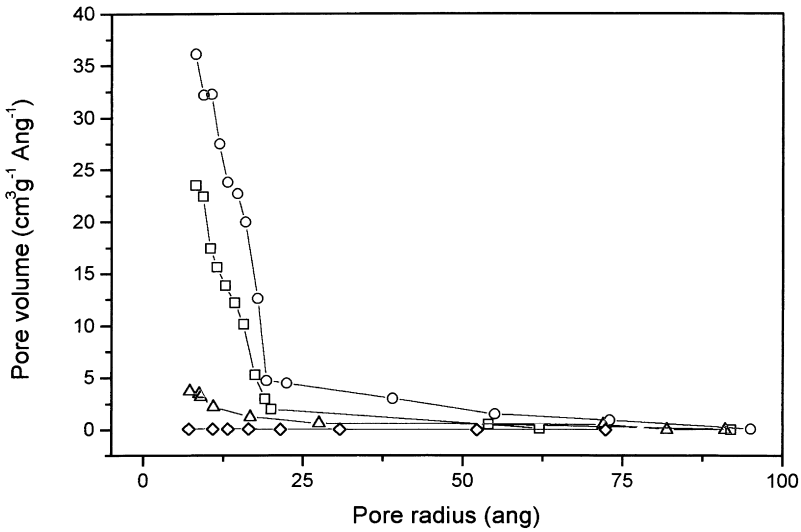

Fig. 9. Pore size distribution from the BET for the silica sample doped with 1% CuCl at (□) 110°C; (○) 500°C; (△) 900°C; and (△) 1100°C.

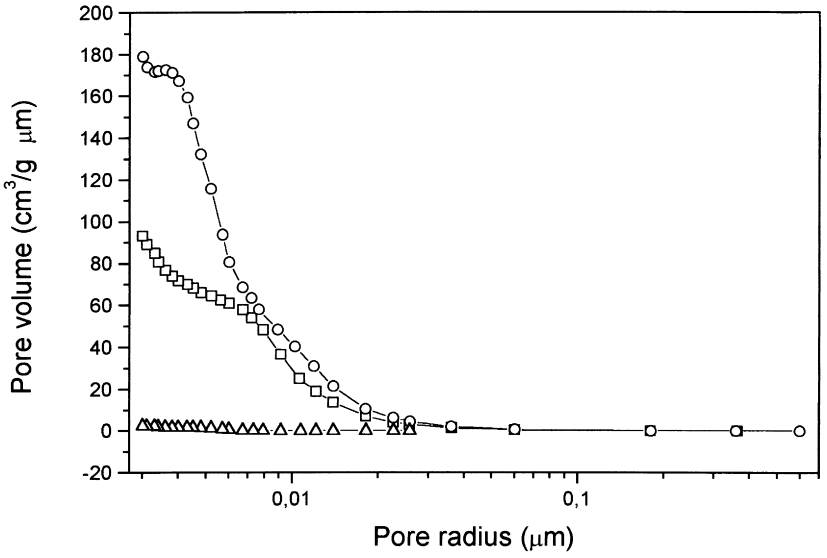

Fig. 10. Pore size distribution for the silica by mercury porosimetry at (□) 110°C; (○) 500°C; and (△) 900°C.

lost weight. Despite this weight loss in the material, this temperature range provokes little shrinkage. Consequently, the density decreases, considering that the weight loss is more significant than the shrinkage at this temperature. Once the organics are eliminated in the network, the increase of the free volume contributes to the increase of the porosity and the solid–pore interface, which can be verified in Fig. 7. Beyond 500°C, the samples began densification as the pores gradually collapsed with the increasing temperature, causing high shrinkage in the samples. Values of the porosity obtained by the mercury porosimetry confirm this behavior, that is, the materials present maximum porosity at 500°C, which suggests a large amount of the free volume in the gel networks.

The surface area of the samples dried at 110°C is approx. 350 m^2/g. Although an increase of the surface area is observed at 500°C, it decreases significantly at 900°C and above. With the aid of the Autosorb program, it is possible to separate the contributions of the micropore area and the mesopore area to the total surface area. It is important to note that pores with openings not exceeding 20 Å are called micropores, and sizes between 20 and 500 Å are called mesopores. Table 3 shows the contributions of these two ranges of pore size for the different samples.

These results show that there is a significant contribution of mesopores in the material dried at 110°C. As the firing temperature increases from 500°C on, the surface area due

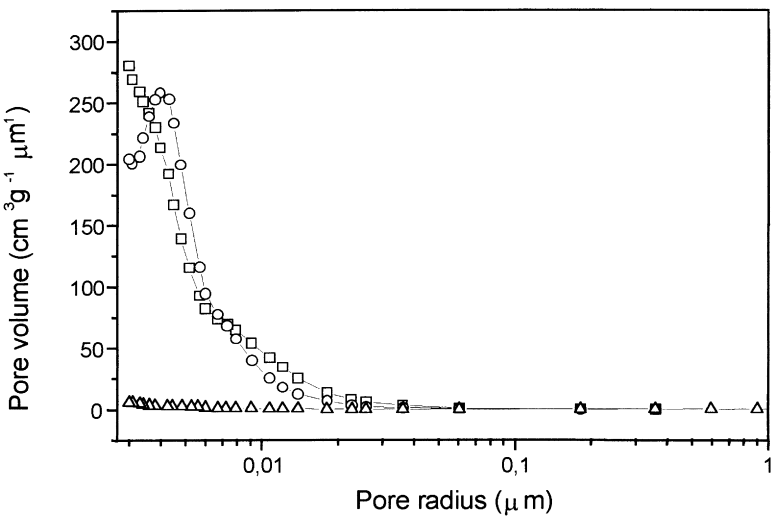

Fig. 11. Pore size distribution for the silica sample doped with 5% CuCl by mercury porosimetry at (□) 110°C; (○) 500°C; and (△) 900°C.

the presence of micro and mesopores decreases, but the contribution of the mesopore area to the total surface becomes progressively bigger. These results can be attributed to the large number of micropores present in the samples treated at low temperature. As the sample is heated from 900°C, a large decrease of the micropore volume in the gel occurs, without altering significantly the amount of the mesopore.

The distribution of pore volume of the different materials with respect to pore size obtained by BET (Figs. 8 and 9) presents some important features. The average pore size of all samples treated up to 900°C is very small, ranging from 12 to 17 Å, and approximately 5 Å for those treated at 1100°C. Equally important, the distribution is very narrow with the maximum value not exceeding 80 Å. That is, the mesopores present in the material are only 5 times the size of the average micropore. Mercury porosimetry confirms this fact. Samples containing pore sizes above 30 Å can be analyzed via this technique. The behavior was similar for all the samples.

By analyzing the results obtained by mercury porosimetry for the different materials, it is observed that for those for pure silica, the variation in the pore size distribution occurs in such a way that the total volume of pores decreases while the average pore size remains fairly constant, around 50 Å, as densification proceeds. At 900°C the samples suffer a strong densification process, according to Fig. 10.

The samples doped with different salt content behave similarly to the matrix. This presents an average pore size of approx. 60 Å, and a strong drop of the pore volume occurs at 900°C. These results can be observed in Fig. 11.

This behavior was similar for all the samples doped with different copper contents. However, the values of the density and surface area are different for each sample. The difference in the densification process can be attributed to differences in the degree of crosslinking that occurred as a result of the combination of the silanol groups (Si-OH) on the pore surface with the liberation of H_2O and the formation of Si–O–Si bonds.

Molecular water can be removed at relatively a low temperature, but hydroxyl groups were only removed in the range 800–1000°C. It was observed that the gel bloated or cracked into fine pieces around 800°C when heating was performed as initially proposed. This suggests that there is a critical temperature for water removal at approx. 800°C.

The proposed procedure for the heat treatment from 900 to 1100°C (heating rate of 10°C/min from 150°C) leads to closure of the pores with trap water, organic residues, and carbon causing bloating. In this way, careful heat treatment around this temperature was conducted to try to obtain bulk glass.

4. Conclusions

A sol–gel process has been successfully employed to prepare Cu-doped silica gels. EVMP, BET and mercury porosimetry provided suitable data for characterization of the samples studied and proved to be complementary techniques used to better understand the structural evolution of these materials.

As the positron probe is able to investigate all the pores, even though not connected to the surface of the crystals, and particularly the narrow pores, the average pore radius measured by PALS is the lowest among these three techniques. The shrinkage of the pores observed by BET and mercury porosimetry at 900°C and further at 1100°C transforms the large pores into little free volumes of nearly 2 Å or less. This appears to be more efficient at inducing Ps formation when compared with the large pores, considering the higher o-Ps intensity observed at the higher firing temperature. This conclusion implies that Ps is formed inside the silica particles and then migrates toward the pores, where it survives.

The XRD patterns indicate that for the samples prepared from $CuSO_4$, the formation of CuO occurs at 900°C and the evolution to Cu_2O at 1100°C. In the case of CuCl samples, it occurs only after the formation of CuO at 900 and 1100°C. For temperatures lower than 500°C, an amorphous material is formed. The data showed the significant evolution for the crystalline phases of the silica of cristobalite and quartz at 1100°C.

Acknowledgements

This work has been supported by CNPq, FAPEMIG and PADCT. The authors thank Walter de Brito of CDTN/CNEN for the XRD measurements.

References

[1] L.L. Hench, J.K. West, The sol–gel process, Chem. Rev. 9 (1990) 33.
[2] C.J. Brinker, G.W. Scherer, Sol–Gel Science. Academic Press, San Diego, CA, 1990, p. 908.
[3] M. Toki, S. Miyashita, T. Takeuchi, S. Kanbe, A. Kochi, A large-size silica glass produced by a new sol-gel process, J. Non-Crystalline Solids 100 (1988) 482.
[4] J.L. Nogues, W.V. Moreshead, Porous gel-silica, a matrix for optically active components, J. Non-Crystalline Solids 121 (1990) 142.
[5] W.W. Adams, S. Kumar, Structure processing of advanced materials, in: D.R. Ulhmann, D.R. Ulrich (Eds.), Conventional and Molecular Composites—Past, Present, and Future, 1st ed., Wiley-Interscience, New York, 1992.
[6] A.J. Rouco, TPR study of Al_2O_3- and SiO_2-supported $CuCl_2$ catalysts, Appl. Catalysts A: General 117 (1994) 149.
[7] A.K. Neyestanaki, N. Kumar, L.E. Lindfors, Catalytic combustion of propane and natural gas over Cu and Pd modified ZSM zeolite catalysts, Appl. Catalysts B: Environmental 7 (1995) 111.
[8] F.Th. van de Scheur, et al., Structure–activity relation and ethane formation in the hydrogenolysis of methyl acetate on

silica supported copper catalysts, Appl. Catalysts A: General 111 (1994) 77.
[9] E. Duval, et al., Magnetic properties of Cu-doped porous silica gels study by magnetic resonances, J. Non-Crystalline Solids 189 (1995) 101.
[10] M. Nogami, Y.Q. Zhu, Y. Tohyama, K. Nagaska, Preparation and nonlinear optical properties of quantum-sized CuCl-doped silica glass by the sol–gel process, J. Am. Ceram. Soc. 74 (1991) 240.
[11] D. Kundu, I. Honma, T. Osawa, H. Komiyama, Preparation and optical nonlinear property of sol-gel derived Cu-SiO_2 thin films, J. Am. Ceram. Soc. 77 (1994) 1112.
[12] Y.C. Jean, Microchem. J. 42 (1990) 72.
[13] R.G. Sousa, R.F.S. Freitas, W.F. Magalhães, Structural characterization of poly(*N*-isopopylacrylamide) gels and some of their copolymers with acrylamide through positron annihilation lifetime spectroscopy. Polymer, 39 (1998) 3815.
[14] D.M. Scharader, Y.C. Jean, Positron and positronium chemistry, in: Studies in Physical and Theoretical Chemistry. Elsevier, Oxford, 1988, p. 57.
[15] J.C. Machado, et al., Positronium formation and inhibition in binary solid solutions on Al(III) and Co(III) tris(acetylacetonates), Chem. Phys. 170 (1993) 263.
[16] P. Kirkegaard, et al., J. Comp. Comm. 23 (1981) 307.
[17] E.M.B. Sousa, Preparação e caracterização de nanocompósitos de sílica dopados com cobre e titânio preparados pelo método sol–gel. Doctorate Thesis. EEUFMG, Belo Horizonte, Brazil, 1997.